Emergent structure in a dipolar Bose gas in a one-dimensional lattice

Ryan M. Wilson and John L. Bohn

JILA and Department of Physics, University of Colorado, Boulder, Colorado 80309-0440, USA

We consider an ultracold dipolar Bose gas in a one-dimensional lattice. For a sufficiently large lattice recoil energy, such a system becomes a series of nonoverlapping Bose-Einstein condensates that interact via the long-range dipole-dipole interaction (ddi). We model this system via a coupled set of nonlocal Gross-Pitaevskii equations (GPEs) for lattices of both infinite and finite extent. We find significantly modified stability properties in the lattice due to the softening of a discrete roton-like mode, as well as "islands" in parameter space where biconcave densities are predicted to exist and that only exist in the presence of the other condensates on the lattice. We solve for the elementary excitations of the system to check the dynamical stability of these solutions and to uncover the nature of their collapse. By solving a coupled set of GPEs exactly on a full numeric grid, we show that this emergent biconcave structure can be realized in a finite lattice with atomic ^{52}Cr.

I. INTRODUCTION

Recent progress on the experimental realization of ultra-cold dipolar quantum fluids is providing an unprecedented opportunity to study these systems in detail. Interesting dipolar effects have been demonstrated in systems with modest dipolar interactions, such as Bose-Einstein condensates (BECs) of ^{52}Cr [1,2]. Additionally, the achievement of a near-quantum-degenerate gas of fermionic ^{40}K^{87}Rb [3], the transfer of bosonic ^{41}K^{87}Rb into its rovibrational ground state [4] and the cooling and trapping of atomic Dy [5] shows promise of a rich future for this field as these species host large dipole moments that may demonstrate new physics both in the mean-field regime and beyond.

Because of the anisotropic nature of the dipole-dipole interaction (ddi), the physics of a dipolar system depends strongly on the geometry of the trap in which it is held. For example, inelastic scattering processes of both bosonic and fermionic species are predicted to be highly suppressed in tighter, quasi-two-dimensional (q2D) traps when the trap is applied along the polarization axis of the dipoles [6–10]. This suppression leads to more stable, longer-lived many-body systems of reactive species. Additionally, it was shown using a BEC of atomic ^{52}Cr that tighter confinement in the polarization direction energetically stabilizes a dipolar BEC (DBEC) against collapse [11]. Thus, tight trapping along the polarization axis is necessary to obtain stable, high-density dipolar quantum fluids.

Such a trap is realizable in a one-dimensional (1D) optical lattice, where a laser is reflected onto itself and high- and low-intensity regions are formed by its interference pattern. The presence of the lattice brings up an interesting point regarding the physics of such a system. While the ddi is anisotropic, it is also long range, scaling as $1/r^3$, and if the lattice spacing is sufficiently small then the effect of the ddi is non-negligible between the lattice sites. For example, interlayer superfluidity is predicted to exist in two adjacent layers of polar fermions [12], and scattering in the 2D plane is predicted to be significantly modified by the presence of a weakly bound state of dipoles in adjacent layers [13]. Dramatic effects are predicted for layers of bosons as well, for both q2D [14,15] and radially trapped [16,17] lattice sites. The

presence of the lattice is predicted to significantly alter the dispersion via the softening of a roton-like mode in the system, and thus to alter the stability properties of the Bose gas.

In this work, we consider a gas of bosonic dipoles in a 1D lattice with the dipoles polarized along the lattice axis so that the system is cylindrically symmetric. Assuming that the lattice recoil is sufficiently large, we model the potentials of the individual sites as cylindrically symmetric harmonic traps. At ultracold temperatures, this leads to a lattice of nonoverlapping DBECs coupled by the long-range ddi. We study the stability of this system both for an infinite and finite 1D lattice. Additionally, we find regions in parameter space where a biconcave structure is predicted to exist that is emergent in the lattice system; in other words, that does not exist in a single condensate. To ensure the accuracy of our results, we calculate the elementary excitations of the system and use them to determine whether our solutions are dynamically stable. In so doing, we map the structure and stability of a 1D lattice of purely dipolar DBECs.

II. FORMALISM

We consider an ultracold dilute gas of bosonic dipoles in a 1D optical lattice in the z direction with lattice spacing d_{lat}. If the lattice is sufficiently deep, it can be modeled by a series of N_{lat} harmonic traps, where each site is described by a cylindrically symmetric potential $U_j(\mathbf{r}) = \frac{1}{2}M\omega_\rho^2[\rho^2 + \lambda^2(z - jd_{\text{lat}})^2]$, where M is the mass of the individual bosons and $\lambda = \omega_z/\omega_\rho$ is the trap aspect ratio. This system is well-described by the coupled set of nonlocal Gross-Pitaevskii equations (GPEs):

$$\left[\hat{h}_j(\mathbf{r}) + \sum_{j'=1}^{N_{\text{lat}}} \phi_d^{j'}(\mathbf{r}) - \mu_j \right] \Psi_j(\mathbf{r}) = 0, \qquad (1)$$

where $\hat{h}_j(\mathbf{r})$ is the noninteracting or single-particle Hamiltonian

$$\hat{h}_j(\mathbf{r}) = -\frac{\hbar^2}{2M}\nabla^2 + U_j(\mathbf{r}), \qquad (2)$$

$\Psi_j(\mathbf{r})$ is the condensate wave function at site j, j is an integer, and μ_j is the corresponding chemical potential. Without the

presence of the long-range ddi, these N_{lat} equations would be independent. The ddi couples the equations through the mean-field potentials $\phi_d^j(\mathbf{r})$ given by the convolution

$$\phi_d^j(\mathbf{r}) = \int d\mathbf{r}' V_d(\mathbf{r} - \mathbf{r}') n_j(\mathbf{r}'), \qquad (3)$$

where $n_j(\mathbf{r}) = |\Psi_j(\mathbf{r})|^2$ is the density of the condensate occupying the jth site with norm $\int d\mathbf{r}' n_j(\mathbf{r}') = N_j$, N_j is the condensate number for site j, and $V_d(\mathbf{r} - \mathbf{r}')$ is the two-body ddi potential for dipoles polarized along $\hat{\mathbf{z}}$, given by [18]

$$V(\mathbf{r} - \mathbf{r}') = d^2 \frac{1 - 3\cos^2\theta_{\mathbf{r}-\mathbf{r}'}}{|\mathbf{r} - \mathbf{r}'|^3}, \qquad (4)$$

where d is the dipole moment of the bosons and $\theta_{\mathbf{r}-\mathbf{r}'}$ is the angle between $\mathbf{r} - \mathbf{r}'$ and $\hat{\mathbf{z}}$. A description of the fully condensed stationary state of this system of dipolar Bose-Einstein condensates (DBECs) is then given by the set of solutions $\{\Psi_j(\mathbf{r}), \mu_j\}$ that minimize the energy functional corresponding to Eq. (1), given by

$$E[\{\Psi_j(\mathbf{r})\}] = \sum_j \int d\mathbf{r} \, \Psi_j^\star(\mathbf{r}) \left[\hat{h}_j(\mathbf{r}) + \frac{1}{2} \sum_{j'=1}^{N_{\text{lat}}} \phi_d^{j'}(\mathbf{r}) \right] \Psi_j(\mathbf{r}). \tag{5}$$

Generally, a full description of a dilute BEC of interacting atoms includes contact interactions given by the pseudopotential $V_c(\mathbf{r} - \mathbf{r}') = g\delta(\mathbf{r} - \mathbf{r}')$ where $g \propto a_s$ and a_s is the s-wave scattering length of the atoms. This interaction is short range and results in the mean-field potential $\phi_c^j(\mathbf{r}) = g|\Psi_j(\mathbf{r})|^2$. Modeling a system of nonoverlapping BECs in a 1D lattice interacting only via contact interactions results in a set of uncoupled GPEs. While the interplay of contact and dipole-dipole interactions is predicted to produce interesting effects [19] that would likely be modified by the presence of the lattice, we set $a_s = 0$ in this work to illuminate purely dipolar effects. Because of its long-range nature, the ddi does not produce a simple mean field like the contact interaction and requires particular attention.

In practice, the dipolar mean field is calculated in k space to eliminate the problems associated with the divergence of the ddi in real space. To do this, the Fourier transforms of the densities $n_j(\mathbf{r})$ and the ddi $V_d(\mathbf{r} - \mathbf{r}')$ must be calculated. Taking $\mathcal{F}$ to be the Fourier transform operator,

$$\tilde{n}_j(\mathbf{k}) = \mathcal{F}\left[n_j(\mathbf{r})\right] \equiv \int d\mathbf{r} \, n_j(\mathbf{r}) e^{-i\mathbf{k}\cdot\mathbf{r}}. \qquad (6)$$

Here, it will prove useful to define the shifted densities $\nu_j(\mathbf{r}) = n_j(\mathbf{r}_j)$ where $\mathbf{r}_j = \{\rho, z - jd_{\text{lat}}\}$, so that all $\nu_j(\mathbf{r})$ are formally centered about the origin. Then, $\nu_j(\mathbf{r}_{-j}) = n_j(\mathbf{r})$, and we can write $\tilde{n}_j(\mathbf{k}) = \mathcal{F}[\nu_j(\mathbf{r}_{-j})]$. With some simple manipulation, this expression reduces to

$$\tilde{n}_j(\mathbf{k}) = \mathcal{F}[\nu_j(\mathbf{r})] e^{ik_z d_{\text{lat}} j}. \qquad (7)$$

Thus, the k-space density of the DBEC at site j can be rewritten as the Fourier transform of $n_j(\mathbf{r})$ translated into the local set of coordinates, with an additional exponential term accounting for this spatial translation. Now, by the convolution theorem,

the mean-field contribution from the DBEC at site j can be written as

$$\phi_d^j(\mathbf{r}) = \mathcal{F}^{-1}[\tilde{V}_d(\mathbf{k})\tilde{n}_j(\mathbf{k})] \qquad (8)$$

where $\tilde{V}_d(\mathbf{k})$ is the Fourier transform of the ddi [20]:

$$\tilde{V}_d(\mathbf{k}) = \frac{4\pi\hbar^2 a_{dd}}{M}\left(3\frac{k_z^2}{k^2} - 1\right) \qquad (9)$$

and $a_{dd} = \frac{Md^2}{3\hbar^2}$ is the characteristic dipole length. In this work, we calculate $\nu_j(\mathbf{r})$ directly by calculating the shifted condensate wave functions $\Phi_j(\mathbf{r})$ such that $\nu_j(\mathbf{r}) = |\Phi_j(\mathbf{r})|^2$ and account for the spatial separation of the DBECs, or the presence of the lattice, with the expression given in Eq. (7). Thus, the wave functions $\Psi_j(\mathbf{r})$ and $\Phi_j(\mathbf{r})$ are related by $\Phi_j(\mathbf{r}) = \Psi_j(\mathbf{r}_j)$.

III. WAVE-FUNCTION ANSATZ

For a single DBEC, calculating the mean-field energy on a full numeric grid has proven fruitful [21,22]; however, this method is computationally very expensive when considering multiple interacting DBECs, both in real space and in k space. In real space, the convolution integral for the dipole-dipole mean field must be done directly, where there is no $1/r^3$ divergence if the condensates do not overlap. In k space, the grid must be large enough to resolve the entire lattice because of the $e^{ik_z d_{\text{lat}} j}$ dependence of the k-space densities. To avoid these problems, we consider solutions of the form $\Phi_j(\mathbf{r}) = \psi_j(\rho)\chi_j(z)$, where

$$\chi_j(z) = \frac{1}{\sqrt{1 + A_{2,j}^2}}[\chi_{0,j}(z) + A_{2,j}\chi_{2,j}(z)], \qquad (10)$$

$$\chi_{0,j}(z) = \frac{1}{\sqrt{l_{z,j}}\pi^{\frac{1}{4}}} \exp\left[-\frac{z^2}{2l_{z,j}^2}\right], \qquad (11)$$

and

$$\chi_{2,j}(z) = \frac{1}{2\sqrt{2l_{z,j}}\pi^{\frac{1}{4}}} \exp\left[-\frac{z^2}{2l_{z,j}^2}\right] H_2\left(\frac{z}{l_{z,j}}\right), \qquad (12)$$

where $H_2(x) = 4x^2 - 2$ is the second Hermite polynomial. This ansatz includes the zeroth and second harmonic oscillator wave functions with variable width and relative amplitude. Plugging this ansatz into the GPE and integrating out the z dependence results in a modified GPE in the radial coordinate ρ that also depends on the widths $l_{z,j}$ and the relative amplitudes $A_{2,j}$ of the axial wave functions, but not the z coordinate explicitly. We derive this modified GPE for a single DBEC, given by Eq. (A2), in Appendix.

To test the ansatz given in Eq. (10), we apply it to the well-known system of a single DBEC in a harmonic trap. This system was predicted to exhibit, for certain trap geometries and ddi strengths, biconcave structures where the maximum density of the DBEC exists not in the center of the trap, but in a ring about the center of the trap [23]. For example, such structure is predicted to exist in a trap with aspect ratio $\lambda = 7$ for ddi strengths near the stability threshold.

Figure 1 compares the total energies of a single DBEC in a trap with $\lambda = 7$ as a function of the ddi strength $(N-1)g_d/a_\rho$, where $a_\rho = \sqrt{\hbar/(M\omega_\rho)}$ is the radial harmonic oscillator length
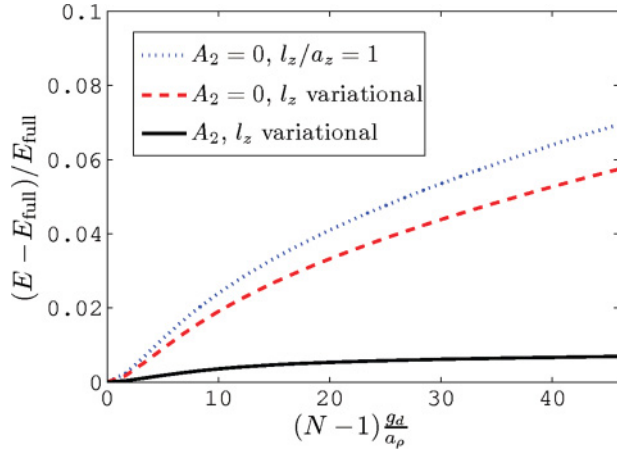
FIG. 1. (Color online) Differences in energy of a DBEC in a trap with aspect ratio $\lambda = 7$ as a function of interaction strength between that calculated using the ansatz given in Eq. (10) and that calculated exactly on a full numeric grid. The blue dotted line shows the energy difference calculated using no second-order harmonic-oscillator wave function and a fixed axial width $l_z = a_z$, the red dashed line shows the energy difference using the same wave function but with l_z treated variationally and the black solid line shows the energy difference including the second-order harmonic-oscillator wave function where the relative amplitude A_2 and l_z are treated variationally.

and $g_d = \frac{2\sqrt{2\pi}\hbar^2 a_{dd}}{M}$ is the ddi coupling, for various restrictions placed on the variational parameters of the axial wave function. Plotted is the energy difference $(E - E_{\text{full}})/E_{\text{full}}$, where E_{full} is the energy calculated by solving the GPE exactly (within strict numerical precision) on a full numeric grid in ρ and z. The blue dotted line shows the energy of the DBEC when $A_2 = 0$ and l_z is fixed to be the axial harmonic oscillator length, $a_z = \sqrt{\hbar/(M\omega_z)}$, the red dashed line shows the energy when $A_2 = 0$ and l_z is treated variationally, and the black line shows the energy when A_2 and l_z are both treated variationally. Clearly, the full variational treatment is much more accurate than the cases where the second harmonic-oscillator wave function is not included ($A_2 = 0$). Indeed, it stays within 1% of the exact energy for all values of $(N - 1)g_d/a_\rho$ for which the DBEC is stable. We find this to hold true for larger trap aspect ratios as well. Figure 2 shows the values of the variational parameters for the same cases as in Fig. 1. In this figure, the left vertical axis is labeled l_z/a_z and the right vertical axis is labeled A_2, shown by the black dots.

Beyond energetics, this ansatz also predicts semiquantitatively the structure and stability of a single DBEC. An interesting feature of the biconcave structure predicted in Ref. [23] is that it exists in "islands" of parameter space defined by $(N - 1)g_d/a_\rho$ and λ. Figure 3 shows this structure- stability diagram for a single DBEC calculated using (a) $A_2 = 0$ and $l_z/a_z = 1$, (b) A_2 and l_z variational, and (c) a full numeric grid in ρ and z. Interestingly, the biconcave islands are present in each diagram and occur for almost exactly the same values of $(N - 1)g_d/a_\rho$. They are, however, shifted in λ, moving to smaller values as more restrictions are placed on the condensate wave function. The diagram for the full variational ansatz (b) qualitatively matches that of the
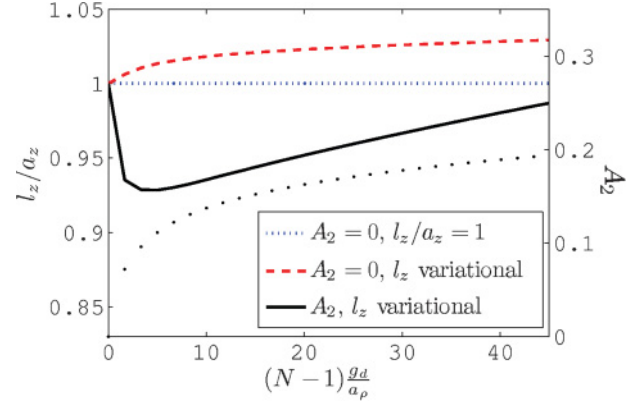

FIG. 2. (Color online) The values of the axial wave-function parameters that, together with the radial wave function calculated on a grid, minimize the energy of a single DBEC in a trap with aspect ratio $\lambda = 7$. The blue dotted line shows the results for $l_z = a_z$, the red dotted line shows l_z when it is treated variationlly and $A_2 = 0$, and the black solid line shows l_z when both it and A_2 are treated variationally. In this last case, the behavior of A_2 is given by the black dotted line.

full numeric grid. Thus, we expect that this ansatz will give physically meaningful results, if not quite quantitative ones.

As we discuss below, a key benefit of this ansatz for the 1D lattice system is that it is analytic in z. Another such ansatz that has this property is that of correlated Gaussians, which have been shown to reproduce the results of full numeric calculations for DBECs quite well [24]. However, we applied this ansatz to the lattice system and found that it is numerically unstable with the minimization techniques used here.

IV. INFINITE LATTICE

With confidence in the ansatz given in Eq. (10), we now apply it to the 1D lattice system. An interesting example to consider is that of an infinite lattice with $N_{\text{lat}} \to \infty$. This approximation introduces a discrete invariance to the system so that we can set $\Phi_j(\mathbf{r}) = \Phi_{j'}(\mathbf{r})$ for all j, j'. Thus, we can neglect, for the time being, the indexing of the wave functions
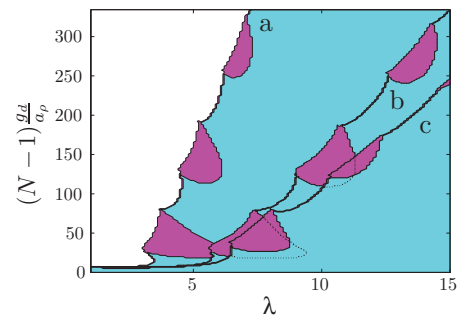

FIG. 3. (Color online) Structure-stability diagram for a single DBEC. The colored regions indicate a dynamically stable condensate, and the pink (darker) regions indicate parameters for which the DBEC has biconcave density. (a) and (b) are calculated using the ansatz for the axial wave function given in Eq. (10) and (c) is calculated using a full numeric grid. For (a), $A_2 = 0$ and $l_z/a_z = 1$ and, for (b), A_2 and l_z are treated variationally.

and let $\Phi_j(\mathbf{r}) \to \Phi(\mathbf{r})$ for all j. Then, the mean-field potential at any site is, from Eq. (7), given by

$$\phi_d(\mathbf{r}) = \sum_{j=-\infty}^{\infty} \int d\mathbf{k} \, \tilde{V}_d(\mathbf{k}) \tilde{n}(\mathbf{k}) e^{ik_z d_{\text{lat}} j} e^{-i\mathbf{k}\cdot\mathbf{r}}, \quad (13)$$

where

$$\tilde{n}(\mathbf{k}) = \tilde{n}_\rho(k_\rho) \frac{e^{-\frac{1}{4}k_z^2 l_z^2}}{1 + A_2^2} \left\{ 1 + A_2 \left[A_2 \right. \right.$$
$$\left. \left. - \left(\frac{1}{\sqrt{2}} + A_2 \right) k_z^2 l_z^2 + \frac{1}{8} A_2 k_z^4 l_z^4 \right] \right\}. \quad (14)$$

We can manipulate the infinite sum in Eq. (13) to give [25]

$$\sum_{j=-\infty}^{\infty} e^{ik_z d_{\text{lat}} j} = \frac{2\pi}{d_{\text{lat}}} \sum_{j=-\infty}^{\infty} \delta\left(k_z - \frac{2\pi j}{d_{\text{lat}}} \right). \quad (15)$$

The term that accounts for the infinite lattice can therefore be written as a Dirac comb in k_z with spacing $2\pi/d_{\text{lat}}$ between peaks. Inserting this expression into Eq. (13) gives the mean-field potential

$$\phi_d(\mathbf{r}) = 2 \frac{g_d}{d_{\text{lat}}} \mathcal{F}_{2D}^{-1}[F_{\text{inf}}(k_\rho) \tilde{n}_\rho(k_\rho)], \quad (16)$$

where $2g_d F_{\text{inf}}(k_\rho)/d_{\text{lat}}$ is the effective k-space ddi for the infinite lattice and $F_{\text{inf}}(k_\rho)$ is given by

$$F_{\text{inf}}(k_\rho) = \sqrt{\frac{\pi}{2}} \sum_{j=-\infty}^{\infty} \frac{e^{-2\pi^2 j^2 \frac{l_z^2}{d_{\text{lat}}^2}}}{(1 + A_2^2)^2} \left\{ 1 + A_2 \left[A_2 \right. \right.$$
$$\left. \left. - \left(\frac{1}{\sqrt{2}} + A_2 \right) 4\pi^2 j^2 \frac{l_z^2}{d_{\text{lat}}^2} + 2A_2 \pi^4 j^4 \frac{l_z^4}{d_{\text{lat}}^4} \right] \right\}^2$$
$$\times \left(\frac{12\pi^2 j^2}{k_\rho^2 d_{\text{lat}}^2 + 4\pi^2 j^2} - 1 \right). \quad (17)$$

The GPE for an infinite lattice of interacting DBECs is reduced to a single GPE in the radial coordinate ρ where all of the axial dependence of the wave function is captured by the variational parameters A_2 and l_z.

We study the structure and stability of this infinite lattice of interacting DBECs by solving the modified GPE for the system (applying conjugate gradients [26] to minimize the corresponding energy functional) and studying the Bogoliubov–de Gennes (BdG) excitations. We find that the sum in Eq. (17) is sufficiently converged if a cutoff j_{cut} is applied to the index j such that $j_{\text{cut}} \gg d_{\text{lat}}/(2\pi l_z)$.

Consistent with other results [14,15], we find that the presence of the lattice serves to destabilize the system due to the softening of a discrete roton-like mode in the system. For a single DBEC in a trap, tight axial confinement aligns the dipoles so that they are predominately repulsive and, for sufficiently low densities or interactions strengths, stabilizes the condensate. In the presence of a 1D lattice, the attraction from the dipoles at other lattice sites extends the condensate in the axial direction, increasing the integrated axial density and, ultimately, making the system less stable. This destabilization is made less dramatic as d_{lat} is increased.
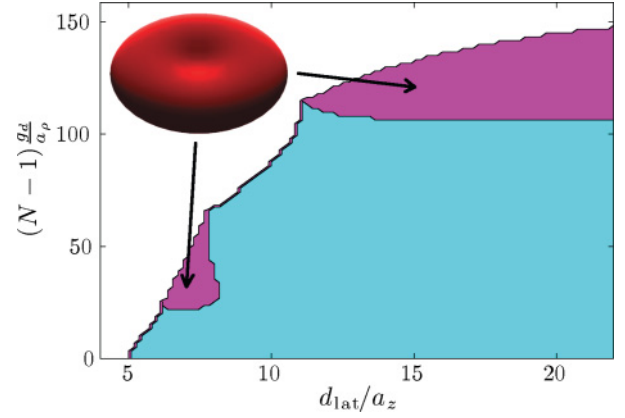

FIG. 4. (Color online) Structure-stability diagram for an infinite lattice of DBECs in traps with aspect ratio $\lambda = 10$ as a function of lattice spacing d_{lat}/a_z and interaction strength $(N-1)g_d/a_\rho$. The colored region indicates dynamic stability, while the pink (darker) regions indicate parameters where the DBECs have biconcave density. The inset shows an isodensity plot of a DBEC with biconcave density.

To study the structure and stability of the infinite lattice, we choose specific trap aspect ratios and explore the parameter space defined by $(N-1)g_d/a_\rho$ and d_{lat}. Figure 4 shows the region of dynamic stability for an infinite lattice of DBECs in traps with $\lambda = 10$. For lattice spacings $d_{\text{lat}}/a_z \lesssim 5$, the condensate wave functions at adjacent sites overlap and the strong dipole-dipole attraction leads to complete instability. In this figure, the colored regions indicate dynamic stability and the pink (dark) regions indicate parameters at which the DBECs exhibit biconcave density. As d_{lat}/a_z is increased, the diagram approaches that given by a line at $\lambda = 10$ in Fig. 3 for a single DBEC. However, for smaller lattice spacings, a second biconcave island appears. Without the presence of the lattice, biconcave structure would not exist for these parameters. Thus, this structure is "emergent" in the lattice system. The inset in Fig. 4 shows an isodensity plot of a DBEC with biconcave density.

Figure 5 shows the region of dynamic stability up to lattice spacings of $d_{\text{lat}}/a_z = 80$ for a infinite lattice of DBECs in harmonic traps with $\lambda = 20$. Here, the convergence of the stability line to $(N-1)g_d/a_\rho \sim 550$ is clear. The inset shows a close-up view of the diagram where a biconcave island is predicted to exist. As the aspect ratio is increased, the values of interaction strength $(N-1)g_d/a_\rho$ that the biconcave islands span becomes relatively smaller compared to the asymptotic value of the stability line. Figure 6 shows the stability lines for infinite lattices with aspect ratios $\lambda = 50, 100, 150$. We find stability islands that exist at the stability threshold within the lattice spacings $d_{\text{lat}}/a_z = 6$ to 10 for all of these aspect ratios. Because they are so narrow in $(N-1)g_d/a_\rho$, though, they are not included in this plot.

By working in the ρ and z coordinates, a cylindrical symmetry is assumed. However, it was shown in [23] that DBECs with biconcave densities are dynamically unstable to angular modes, or quasiparticles. While the method used here is sensitive to dynamic instabilities that are purely radial, an extra step must be taken to detect angular instabilities.
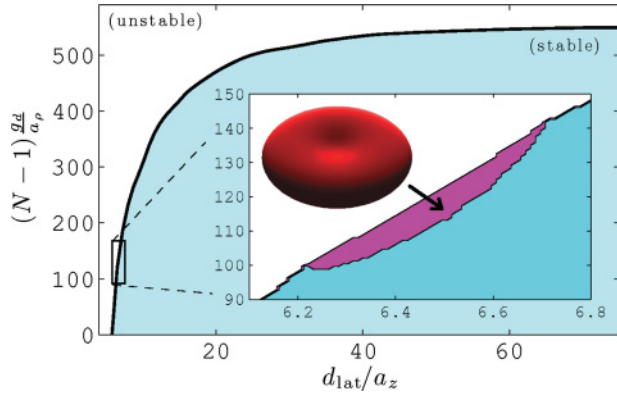
FIG. 5. (Color online) Structure-stability diagram for an infinite lattice of DBECs in traps with aspect ratio $\lambda = 20$ as a function of lattice spacing d_{lat}/a_z and interaction strength $(N-1)g_d/a_\rho$. The inset shows a close-up of the diagram at the parameters indicated. The pink (darker) region in the inset indicates parameters where the DBECs have biconcave density. An isodensity plot of a DBEC with biconcave density is shown in this inset.

A. Bogoliubov–de Gennes equations

The Bogoliubov–de Gennes (BdG) equations describe the low-lying quasiparticles of the condensate. They are derived by inserting the ansatz

$$\psi(\rho) \rightarrow [\psi(\rho) + \delta u(\rho)e^{i(m\varphi-\omega t)} + \delta v(\rho)e^{-i(m\varphi-\omega t)}]e^{-i\mu t} \tag{18}$$

into the time-dependent GPE and linearizing about δ, assuming that $\delta \ll 1$. Here, m is the quantum number describing the projection of angular momentum of the quasiparticle onto the z axis. In general, the energy eigenvalues of the BdG modes $\{u, v^\star\}$ can be written as $\omega = \omega_R + i\omega_I$, where ω_R and ω_I are purely real. When all $\omega_I = 0$, the system is dynamically stable. However, when some $\omega_I \neq 0$, the system is dynamically unstable, and the quasiparticle amplitude grows exponentially in time on a time scale $\sim 1/\omega_I$.

Like the single DBEC in [23], we find that the biconcave structures in the infinite lattice are, for some critical density
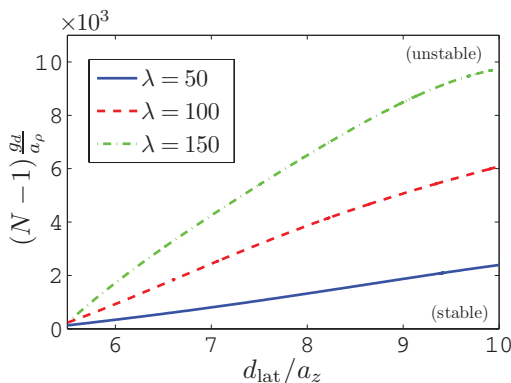

FIG. 6. (Color online) Stability lines for an infinite lattice of DBECs for aspect ratios $\lambda = 50, 100, 150$ as a function of lattice spacing d_{lat}/a_z and interaction strength $(N-1)g_d/a_\rho$. The parameters beneath the lines are dynamically stable, while those above the lines are dynamically unstable.

or ddi, dynamically unstable to angular quasiparticles with $m \geqslant 2$. Reference [21] shows that this angular instability leads to angular collapse, or collapse with angular nodes, of the biconcave DBECs. A measurement of the character of collapse, whether it be radial or angular, then provides a tool to map the structure along the stability threshold of the system.

In our analysis, we found exotic ground-state densities very close to the stability threshold, like those found for a finite lattice in Ref. [16]. These solutions host multiple radial density oscillations; however, we find they are dynamically unstable and are thus unlikely to be experimentally observable.

V. FINITE LATTICE

While the infinite lattice of DBECs provides a clear, simple example of emergent structure in this system, it is a difficult system to realize experimentally. In a realistic experiment, the lattice has a finite extent and the occupations of the sites vary from site to site. To model this more realistic lattice system, we consider an odd number of occupied lattice sites indexed by $j \in [-j_{\text{lat}}, j_{\text{lat}}]$ where $j_{\text{lat}} = (N_{\text{lat}} - 1)/2$ with the particle number given by a Gaussian distribution, $N_j = N_{\text{max}} \exp[-(j/j_{\text{lat}})^2]$, where N_{max} is the particle number in the condensate in the center of the lattice at site $j = 0$, and the outer-most sites have particle number N_{max}/e [16].

Instead of using an analytic form for the axial parts of the condensate wave functions, we solve the coupled set of GPEs given by Eq. (1) on a full grid (large enough to encapsulate the entire lattice) in ρ and z for each condensate. We find good convergence by using the conjugate gradients method to minimize the full energy functional of the system [26]. Additionally, to ensure numerical precision we apply a cutoff to the ddi in ρ and z so that a relatively small grid can be used while eliminating the effects of artificial "image" condensates that are present due to the use of the fast Fourier transform (FFT) algorithm in our calculation [19].

As an example, we consider a lattice with trap aspect ratios $\lambda = 50$, $j_{\text{lat}} = 4$ (corresponding to 9 occupied lattice sites), lattice spacing $d_{\text{lat}} = 8a_z$, and $(N_{\text{max}} - 1)g_d/a_\rho = 550$ on a numeric grid of size $[N_z, N_\rho] = [1024, 128]$. Figure 7 shows the density at $z = 0$ of a DBEC at the center of the lattice ($j = 0$) and, for comparison, the density of a DBEC with the same trap aspect ratio and ddi strength $(N-1)g_d/a_\rho = 550$ but without the presence of the lattice. While the DBEC in the single trap does not exhibit biconcave structure, the DBEC in the lattice does, showing that this emergent structure in the lattice system is present not only in the infinite lattice system, but also in the experimentally realistic system of a finite lattice with variable occupancy. Indeed, such a system is realizable with atomic ^{52}Cr, having a permanent magnetic dipole moment of $\mu = 6\mu_B$ where μ_B is the Bohr magneton, axial harmonic oscillator frequencies of $\omega_z = 2\pi \times 30$ kHz and a maximum condensate occupancy of $N_{\text{max}} \simeq 77 \times 10^3$ atoms.

The experimental observability of biconcave structure in a lattice of DBECs is an important point to address. While nondestructive phase-contrast imaging techniques of trapped condensates have been successful [27], it is questionable whether such techniques can resolve the small differences in the spatial density of the biconcave condensate, especially in a 1D lattice when the other trapped condensates do not
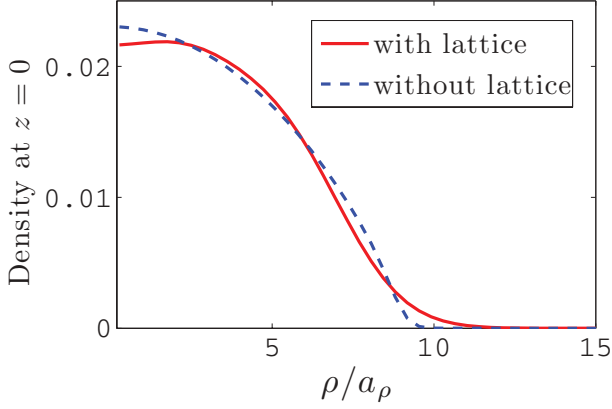
FIG. 7. (Color online) Radial densities at $z = 0$ of a DBEC with $(N-1)g_d/a_\rho = 550$ in a trap with aspect ratio $\lambda = 50$. The blue dashed line shows the density of a DBEC in a single harmonic trap, and the red solid line shows the density of a DBEC in the center site of a 1D lattice with nine occupied sites ($j_{\text{lat}} = 4$). This DBEC exhibits biconcave structure, while the single DBEC does not, demonstrating the emergence of this structure in the lattice system. These densities were calculated by solving the GPE (coupled GPEs) exactly on a full numeric grid.

necessarily exhibit such structure. However, it was shown in Ref. [21] that DBECs with biconcave structure will, at a critical density, collapse anisotropically with nodal structure about the ring of maximum density. This angular character is predicted to be preserved in the expansion of the collapsed state, thereby providing an indirect signature of biconcave structure in the expanded cloud. In a system of DBECs with nonzero scattering lengths, collapse of the system can be induced by decreasing the scattering length below a critical value via a Fano-Feshbach resonance [21].

VI. CONCLUSION

In conclusion, we have mapped the structure and stability of a lattice of interacting, purely dipolar DBECs. By asserting an analytic form for the axial part of the condensate wave functions [Eqs. (10)–(12)], we derive a simple, modified GPE for the radial part of the wave functions when the lattice is infinite. We find isolated regions ("islands") in the parameter space defined by the lattice spacing and the ddi strength where the DBECs are predicted to exhibit biconcave densities, where the maximum density exists not in the center of the trap but in a ring about the center of the trap. To model a more experimentally realistic system, we consider a finite lattice with varying condensate number and solve the coupled set of GPEs exactly on a full numeric grid. In doing so, we show that this emergent biconcave structure should be observable in a finite 1D lattice of DBECs of atomic ^{52}Cr.

APPENDIX: MODIFIED GPE USING ZEROTH AND SECOND HARMONIC-OSCILLATOR WAVE FUNCTIONS

Consider the ansatz given by Eqs. (10)–(12) for a system with a single harmonically trapped DBEC, so the indexing of the condensate wave function can be ignored and we can simply write $\Phi(\mathbf{r}) = \psi(\rho)\chi(z)$. We derive the modified GPE by multiplying the (dimensionless) GPE:

$$\left[-\frac{1}{2}\nabla^2 + U(\mathbf{r}) + \phi_d(\mathbf{r}) - \mu \right] \Phi(\mathbf{r}) = 0, \qquad \text{(A1)}$$

by $\chi(z)$ and integrating over z. This operation gives the modified GPE,

$$\left\{ \hat{h}_{\text{eff}}(\rho) + 2\frac{g_d}{l_z}\mathcal{F}_{2D}^{-1}\left[\tilde{n}_\rho(k_\rho)F_{\text{eff}}\left(\frac{k_\rho l_z}{\sqrt{2}}\right)\right]\right\} \psi(\rho) = 0,$$
$$\text{(A2)}$$

where $\hat{h}_{\text{eff}}(\rho)$ is the effective single-particle Hamiltonian,

$$\hat{h}_{\text{eff}}(\rho) = -\frac{1}{2}\nabla_\rho^2 + \frac{1}{2}\omega_\rho^2\rho^2 - \mu + \frac{1}{1+A_2^2}$$
$$\times \left[\left(\frac{1}{l_z^2}+\lambda^2 l_z^2\right)\left(\frac{1}{4}+\frac{5}{4}A_2^2\right) - \frac{A_2}{\sqrt{2}}\left(\frac{1}{l_z^2}-\lambda^2 l_z^2\right)\right],$$
$$\text{(A3)}$$

and $F_{\text{eff}}(x)$ is given by

$$F_{\text{eff}}(x) = \frac{1}{\left(1+A_2^2\right)^2}\left[1 + \sqrt{2}A_2(3x^2-1) + \frac{3}{4}A_2^2\right.$$

$$\times (3+5x^2+6x^4) + \frac{1}{4\sqrt{2}}A_2^3(1+9x^2+42x^4$$

$$+12x^6) + \frac{1}{64}A_2^4[41+3x^2(81+134x^2+60x^4$$

$$+8x^6)] - \frac{3\sqrt{\pi}}{2}\left\{ 1 + A_2\left[A_2\left(2+A_2^2\right)\right.\right.$$

$$+2(\sqrt{2}+2A_2)\left(1+A_2^2\right)x^2 + A_2\left(3+4\sqrt{2}A_2\right.$$

$$\left. +5A_2^2\right)x^4 + A_2^2(\sqrt{2}+2A_2)x^6 + \frac{1}{4}A_2^3 x^8\right]\right\}$$

$$\left. \times xe^{x^2}\text{Erfc}\,[x]\right], \qquad \text{(A4)}$$

and $\text{Erfc}[x]$ is the complementary error function. The corresponding mean-field energy due to the ddi is then

$$E_d = \frac{g_d}{l_z}\int d^2\rho\, n_\rho(\rho)\mathcal{F}_{2D}^{-1}\left[\tilde{n}_\rho(k_\rho)F_{\text{eff}}\left(\frac{k_\rho l_z}{\sqrt{2}}\right)\right]. \qquad \text{(A5)}$$

[1] T. Lahaye, T. Koch, B. Fröhlich, M. Fattori, J. Metz, A. Griesmaier, S. Giovanazzi, and T. Pfau, Nature (London) **448**, 672 (2007).

[2] T. Lahaye, C. Menotti, L. Santos, M. Lewenstein, and T. Pfau, Rep. Prog. Phys. **72**, 126401 (2009).

[3] K.-K. Ni, S. Ospelkaus, M. H. G. de Miranda, A. P. B. Neyenhuis, J. J. Zirbel, S. Kotochigova, P. S. Julienne, D. S. Jin, and J. Ye, Science **322**, 231 (2008).

[4] K. Aikawa, D. Akamatsu, M. Hayashi, K. Oasa, J. Kobayashi, P. Naidon, T. Kishimoto, M. Ueda, and S. Inouye, e-print arXiv:1008.5034.

[5] M. Lu, S. H. Youn, and B. L. Lev, Phys. Rev. Lett. **104**, 063001 (2010).

[6] G. Quéméner and J. L. Bohn, Phys. Rev. A **83**, 012705 (2011).

[7] J. P. D'Incao and C. H. Greene, e-print arXiv:1011.3469.

[8] A. Micheli, G. Pupillo, H. P. Büchler, and P. Zoller, Phys. Rev. A **76**, 043604 (2007).

[9] G. Quéméner and J. L. Bohn, Phys. Rev. A **81**, 060701 (2010).

[10] A. Micheli, Z. Idziaszek, G. Pupillo, M. A. Baranov, P. Zoller, and P. S. Julienne, Phys. Rev. Lett. **105**, 073202 (2010).

[11] T. Koch, T. Lahaye, J. Metz, B. Fröhlich, A. Griesmaier, and T. Pfau, Nature Phys. **4**, 218 (2008).

[12] A. Pikovski, M. Klawunn, G. V. Shlyapnikov, and L. Santos, e-print arXiv:1008.3264.

[13] M. Klawunn, A. Pikovski, and L. Santos, Phys. Rev. A **82**, 044701 (2010).

[14] M. Klawunn and L. Santos, Phys. Rev. A **80**, 013611 (2009).

[15] D. W. Wang and E. Demler, e-print arXiv:0902.0885.

[16] P. Köberle and G. Wunner, Phys. Rev. A **80**, 063601 (2009).

[17] A. Junginger, J. Main, and G. Wunner, Phys. Rev. A **82**, 023602 (2010).

[18] S. Yi and L. You, Phys. Rev. A **61**, 041604 (2000).

[19] H. Y. Lu, H. Lu, J. N. Zhang, R. Z. Qiu, H. Pu, and S. Yi, Phys. Rev. A **82**, 023622 (2010).

[20] K. Góral and L. Santos, Phys. Rev. A **66**, 023613 (2002).

[21] R. M. Wilson, S. Ronen, and J. L. Bohn, Phys. Rev. A **80**, 023614 (2009).

[22] T. Lahaye, J. Metz, B. Fröhlich, T. Koch, M. Meister, A. Griesmaier, T. Pfau, H. Saito, Y. Kawaguchi, and M. Ueda, Phys. Rev. Lett. **101**, 080401 (2008).

[23] S. Ronen, D. C. E. Bortolotti, and J. L. Bohn, Phys. Rev. Lett. **98**, 030406 (2007).

[24] S. Rau, J. Main, P. Köberle, and G. Wunner, Phys. Rev. A **81**, 031605 (2010).

[25] M. Jeng, Am. J. Phys. **68** (2000).

[26] S. Ronen, D. C. E. Bortolotti, and J. L. Bohn, Phys. Rev. A **74**, 013623 (2006).

[27] M. R. Andrews, M. O. Mewes, N. J. vanDruten, D. S. Durfee, D. M. Kurn, and W. Ketterle, Science **273**, 84 (1996).